IJMGE

Int. J. Min. & Geo-Eng.
Vol.48, No.1, June 2014, pp 55-68.

Analytical Solution for Stress Field and Intensity Factor in CSTBD under Mixed Mode Conditions

Najaf Ali Ghavidel [1*], Hosein Memarian [1], Soheil Mohamadi [2], Mohammad Heydarizadeh[1]

1. School of Mining, College of Engineering, University of Tehran, Iran

2. School of Civil, College of Engineering, University of Tehran, Iran

Received 26 November 2013; Received in revised form 16 January 2014; Accepted 2 May 2014
**Corresponding author: ali.qavidel@ut.ac.ir*

Abstract

Considering the fact that rocks fail faster under tensile stress, rock tensile strength is of great importance in applications such as blasting, rock fragmentation, slope stability, hydraulic fracturing, caprock integrity, and geothermal energy extraction. There are two direct and indirect methods to measure tensile strength. Since direct methods always encompass difficulties in test setup, indirect methods, specifically the Brazilian test, have often been employed for tensile strength measurement. Tensile failure is technically attributed to crack propagation in rock. Fracture mechanics has significant potential for the determination of crack behaviour as well as propagation pattern. To apply Brazilian tests, cracked disc geometry has been suggested by the International Society for Rock Mechanics ISRM. Accordingly, a comprehensive study is necessary to evaluate stress field and stress intensity factor (SIF) around the crack in the centre of the specimen. In this paper, superposition principle is employed to solve the problem of cracked straight-through Brazilian disc (CSTBD), using two methods of dislocation and complex stress function. Stress field and SIF in the vicinity of the crack tip are then calculated. With the proposed method, the magnitude of critical load for crack initiation in structures can be predicted. This method is valid for any crack of any arbitrary length and angle. In addition, numerical modelling has been carried out for the Brazilian disc. Finally, the analytical solution has been compared with numerical modelling results showing the same outcome for both methods.

Keywords: *cracked straight-through Brazilian disc (CSTBD), numerical modelling, stress field, stress intensity factor (SIF), tensile strength.*

1. Introduction

Tensile strength is of great importance in the scope of rock mechanics such as blasting, rock fragmentation, slope stability, hydraulic fracturing, cap rock integrity, and geothermal energy extraction. There are two methods to determine tensile strength, namely the direct

and indirect methods. Indirect methods, specifically the Brazilian test, have often been employed in an effort to determine tensile strength since direct methods always encompass difficulties in test setup.

Crack initiation or microcrack propagation results in rock failure. Rock failure is an important issue in fracture mechanics. For applying Brazilian tests, cracked Brazilian disc geometry has been taken into account by ISRM due to its benefits compared to other geometries. SIF and magnitude of induced stress are necessary factors in crack propagation.

Over the past two decades there has been a great deal of interest and debate on the stress intensity factor and the unique fracture toughness test method suggested by the International Society for Rock Mechanics (ISRM) [1-11]. The two chevron-notched rock fracture specimens, chevron bend (CB) and short rod (SR), recommended by the ISRM [12, 13] and aimed at determining rock Mode I fracture toughness, have a number of practical disadvantages, such as very low loads required to initiate failure at the correct orientation, complicated loading fixtures, and complex sample preparation for CB and SR specimens [1]. The aforementioned methods have also been unsuitable for mixed mode fractures [3, 5]. The cracked chevron-notched Brazilian disc (CCNBD) and the cracked straight-through Brazilian disc (CSTBD) specimen geometries overcome these problems and are also suitable for mixed fracture mode testing [14, 15]. The general case for the cracked Brazilian disc problem is when the sample is loaded diametrically with the crack inclined at an angle of zero to the loading direction [Fig. 1a]. Different combinations of Mode I and Mode II fracture intensities can be obtained simply by changing this angle.

For the special case when $\theta = 0$ the problem is reduced to the Mode I fracture situation. This problem for CSTBD geometry was studied by Rooke and Tweed [16] and Atkinson [17]. Only Rooke and Tweed [16] have considered the long crack case. The mixed mode CSTBD problem was investigated by Awaji and Sato [14] and Atkinson [17]. These authors only studied short crack cases, so that the higher order components describing the crack and the boundary were neglected [6]. Based on investigations, CSTBD has priority over CCNBD. The main reason for proposing CSTBD is that producing a stream crack is easier than a V-shape crack. Additionally a comparison of studies has shown that toughness in CCNBD for a specific rock is much lower than CSTBD [8].

2.Theoretical Solutions for the CSTBD Fracture Problem under Mixed Mode Conditions

Under plane strain conditions, the problem shown in Fig. 1a can be solved by superimposition of the solutions to the following simpler problems:

- Problem 1: a solid Brazilian disc loaded with a pair of diametrical forces P [Fig. 2a];
- Problem 2: problem 1 will create normal and tangential stresses σ_N and σ_T along the part of the diameter $0 < r < a$, $\beta = \pm\pi/2-\theta$ where there is a crack. This crack is normal and tangential stress-free on its surfaces, so therefore σ_N and σ_T have to be reduced to zero. The second problem will be an infinite region with a central crack (length 2a) subjected to surface normal and tangential stresses $-\sigma_N$ and $-\sigma_T$ [Fig. 2b].
- Problem 3: Problem 2 will generate forces $-P_Y$ and P_Y along the circumference line, which is the disc boundary line. Again these stresses need to be cancelled to enforce the stress-free conditions along the disc boundary. Hence, the third problem is also a solid Brazilian disc, identical to that in problem 1, but subjected to boundary forces $-P_X$ and $-P_Y$ instead [Fig. 2c]. This will again set up the normal and tangential stresses along that part of the diameter mentioned in problem 1. Therefore the solution procedure goes back to solve the condition of problem 2. This iteration goes on step by step until the stresses created along the crack surface and the disc boundary are negligible.

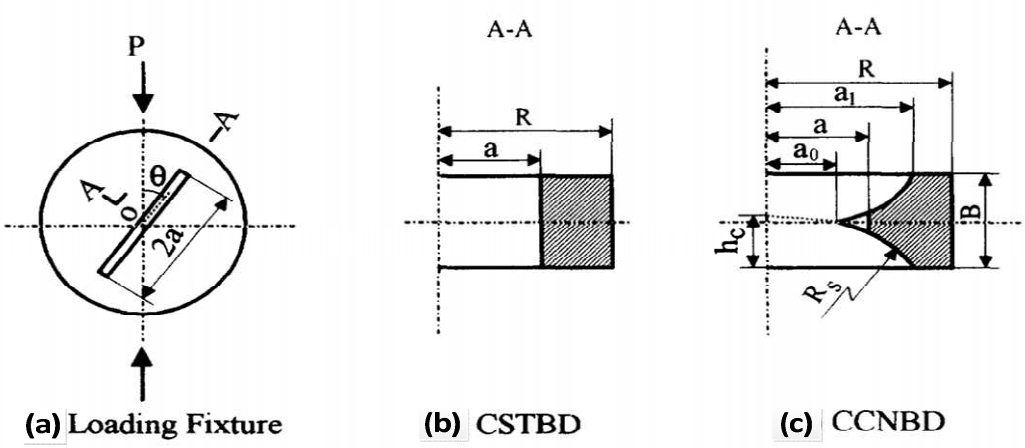

Fig. 1. CSTBD and CCNBD specimen geometries [14].

In this paper, the proposed solution for solving the problem in the first and third method states are discussed; then, the problem is solved and reported in the second state.

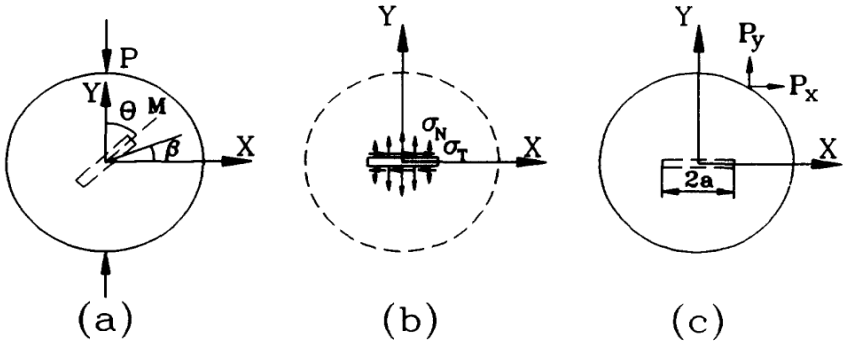

Fig. 2. Solution procedure for the mixed mode CSTBD geometry [6].

We can solve problem 1 from the solution of a solid disc subjected to an arbitrary boundary concentrated force, given by Timoshenko [18]. The derived solutions for the normal and tangential stresses set up along any arbitrary diameter A-A are as follows (Fig. 3):

$$\sigma_N = -\frac{2P\cos\varphi_1}{\pi r_1}\sin^2(\theta+\varphi_1) - \frac{2P\cos\varphi_2}{\pi r_2}\sin^2(\theta+\varphi_2) + \frac{2P}{\pi D}$$

$$\sigma_r = -\frac{2P\cos\varphi_1}{\pi r_1}\cdot\frac{\sin^2[2(\theta+\varphi_1)]}{2} - \frac{2P\cos\varphi_2}{\pi r_2}\cdot\frac{\sin^2[2(\theta+\varphi_2)]}{2} \quad (1a)$$

$$r_1 = \sqrt{a^2.\sin^2\theta + (a.\cos\theta - R)^2} \qquad r_2 = \sqrt{a^2.\sin^2\theta + (a.\cos\theta + R)^2}$$

$$\varphi_1 = \arcsin\frac{a.\sin\theta}{r_1} \qquad \varphi_2 = \arcsin\frac{a.\sin\theta}{r_2} \quad (1b)$$

Similarly we can derive a solution for problem 3 as follows:

$$\sigma_{\mathrm{N}}=\left[\frac{2P_X}{\pi}.\frac{\cos\delta_1}{r_1}+\frac{2P_Y}{\pi}.\frac{\sin\delta_1}{r_1}\right].\sin^2\delta_1+\left[\frac{P_X}{\pi.D}.\sin 2\delta_2+\frac{P_Y}{\pi.D}\sin 2\delta_3\right]$$

$$\sigma_{\mathrm{N}}=\left[\frac{P_X}{\pi}.\frac{\cos\delta_1}{r_1}+\frac{P_Y}{\pi}.\frac{\sin\delta_1}{r_1}\right].\sin 2\delta_1 \tag{2a}$$

where

$$r_1=\sqrt{(x-a)^2+y^2}$$

$$\sin\delta_1=\frac{y}{r_1},\cos\delta_1=\frac{x-s}{r_1} \tag{2b}$$

$$\delta_2=\arctan\frac{x}{y+R},\delta_3=\arctan\frac{y}{x+R}$$

x and y are components of coordinates.

Problem 2 was solved using the dislocation method and a complex stress function method [19]. The stress field within an infinite field with a central crack subjected to arbitrary normal and tangential surface stresses can be calculated by the following expressions:

$$\sigma_{xx}=\int_{-\frac{\pi}{2}}^{\frac{\pi}{2}}\left[\frac{F(\varphi).(x-a\sin\varphi).[y^2-(x-a\sin\varphi)^2]-G(\varphi).y.[3(x-a\sin\varphi)^2+y^2]}{[(x-a\sin\varphi)^2+y^2]^2}\right].d\varphi$$

$$\sigma_{yy}=\int_{-\frac{\pi}{2}}^{\frac{\pi}{2}}\left[\frac{-F(\varphi).(x-a\sin\varphi).[3y^2+(x-a\sin\varphi)^2]+G(\varphi).y.[(x-a\sin\varphi)^2-y^2]}{[(x-a\sin\varphi)^2+y^2]^2}\right].d\varphi \tag{3}$$

$$\sigma_{xy}=\int_{-\frac{\pi}{2}}^{\frac{\pi}{2}}\left[\frac{F(\varphi).y.[y^2-(x-a\sin\varphi)^2]+G(\varphi).(x-a\sin\varphi).[(x-a\sin\varphi)^2-y^2]}{[(x-a\sin\varphi)^2+y^2]^2}\right].d\varphi$$

where $F(\varphi)$ and $G(\varphi)$ are the introduced dislocation densities, simulating the Mode I and Mode II fracture situations, respectively. They can be calculated by the following integration equations:

$$\begin{bmatrix}F(\varphi)\\G(\varphi)\end{bmatrix}=\frac{1}{\pi^2}\int_{-a}^{a}\frac{\sqrt{a^2-x^2}}{x-a\sin\varphi}\begin{bmatrix}\sigma_N(x)\\\sigma_T(x)\end{bmatrix}.dx \tag{4}$$

When using the complex stress function method to solve problem 2, the following complex stress functions are used to represent the action of the shear stress on the crack surface (Fig. 4):

$$\phi(Z)=\frac{P-iQ}{4\pi i(Z-s)}\left[\sqrt{\frac{s^2-a^2}{Z^2-a^2}}+1\right],\psi(Z)=\frac{P-iQ}{4\pi i(Z-s)}\left[\sqrt{\frac{s^2-a^2}{Z^2-a^2}}-1\right] \tag{5}$$

which is taken from Erdogan's solution [20] for a central crack subjected to a pair of surface normal and tangential concentrated forces P and Q. Then the stress field at any point within the infinite region can be calculated from the equations given below:

$$\sigma_{xx}+\sigma_{yy}=2\left[\phi(Z)+\overline{\phi(Z)}\right]$$
$$\sigma_{xx}-\sigma_{yy}+2i\sigma_{xy}=2\left[(\overline{Z}-Z).\phi'(Z)-\phi(Z)+\overline{\psi(Z)}\right] \quad (6)$$

Here Z is the complex coordinate $Z=X+iY$. It has been proved that Erdogan's stress function can only express the action of the crack surface tangential force Q but not the normal force P [20].

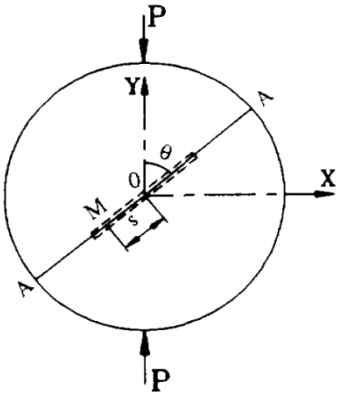

Fig. 3. Solid Brazilian disc [21].

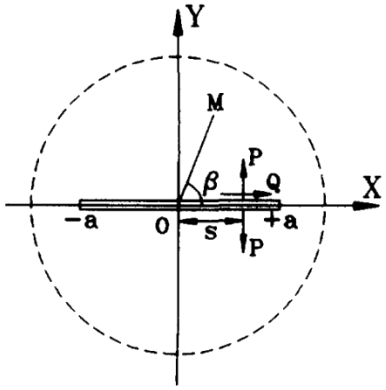

Fig. 4. Complex stress functions [21].

3. Stress Field and Stress Intensity Factor Determination (Mode II) (x=a)

According to Figure 3 and Figure 4, it is assumed in (x=a) such that $Z=a+\xi$, , $\xi=re^{i\theta}$ and $\left|\frac{\xi}{a}\right|<<1$, then:

$$\phi(Z)=\frac{P-iQ}{4\pi i(Z-s)}\left[\sqrt{\frac{s^2-a^2}{Z^2-a^2}}+1\right]=\frac{P-iQ}{4\pi i}\left[\frac{1}{\xi+a-s}.\frac{\sqrt{s^2-a^2}+\sqrt{\xi^2+2a\xi}}{\sqrt{\xi^2+2a\xi}}\right] \quad (7)$$

Considering $\xi\to 0$ at crack tip, therefore power terms of the crack tip would be negligible;

$$\phi(Z)=\frac{P-iQ}{4\pi i}\left[\frac{i}{\sqrt{2a\xi}}\sqrt{\frac{a+s}{a-s}}+\frac{1}{a-s}\right] \quad (8)$$

Substituting $\xi=re^{i\theta}$;

$$\phi(Z)=\frac{1}{4\pi}\left[\frac{P}{\sqrt{2ar}}\sqrt{\frac{a+s}{a-s}}\cos\frac{\theta}{2}-\frac{Q}{\sqrt{2ar}}\sqrt{\frac{a+s}{a-s}}\sin\frac{\theta}{2}-\frac{Q}{a-s}\right]$$
$$-\frac{i}{4\pi}\left[\frac{P}{\sqrt{2ar}}\sqrt{\frac{a+s}{a-s}}\sin\frac{\theta}{2}+\frac{Q}{\sqrt{2ar}}\sqrt{\frac{a+s}{a-s}}\cos\frac{\theta}{2}+\frac{P}{a-s}\right] \quad (9)$$

By differentiating (8) on ξ, it follows:

$$\phi'(Z)=\frac{d\phi}{dZ}=\frac{d}{d\xi}\left\{\frac{P-iQ}{4\pi i}\left[\frac{i}{\sqrt{2a\xi}}\sqrt{\frac{a+s}{a-s}}+\frac{1}{a-s}\right]\right\}=\frac{P-iQ}{4\pi}\left[\frac{-1}{2\sqrt{2a\xi^3}}\sqrt{\frac{a+s}{a-s}}\right] \quad (10)$$

Substituting $\xi=re^{i\theta}$;

$$\phi'(Z)=\frac{-1}{4\pi}\frac{1}{2r\sqrt{2ar}}\sqrt{\frac{a+s}{a-s}}\left[\left(P\cos\frac{3\theta}{2}-Q\sin\frac{3\theta}{2}\right)-i\left(P\sin\frac{3\theta}{2}+Q\cos\frac{3\theta}{2}\right)\right] \quad (11)$$

$\psi(Z)$ is to be solved considering the same condition used for $\phi(Z)$ at (x=a):

$$\psi(Z)=\frac{P-iQ}{4\pi i(Z-s)}\left[\sqrt{\frac{s^2-a^2}{Z^2-a^2}}-1\right]=\frac{P-iQ}{4\pi}\left[\frac{1}{\sqrt{2a\xi}}\sqrt{\frac{a+s}{a-s}}+\frac{i}{a-s}\right] \quad (12)$$

Substituting $\xi,=re^{i\theta}$;

$$\psi(Z)=\frac{1}{4\pi}\left[\frac{P}{\sqrt{2ar}}\sqrt{\frac{a+s}{a-s}}\cos\frac{\theta}{2}-\frac{Q}{\sqrt{2ar}}\sqrt{\frac{a+s}{a-s}}\sin\frac{\theta}{2}+\frac{Q}{a-s}\right]$$
$$-\frac{i}{4\pi}\left[\frac{P}{\sqrt{2ar}}\sqrt{\frac{a+s}{a-s}}\sin\frac{\theta}{2}+\frac{Q}{\sqrt{2ar}}\sqrt{\frac{a+s}{a-s}}\cos\frac{\theta}{2}-\frac{P}{a-s}\right] \quad (13)$$

Here, by substituting values of $\phi(Z)$, $\phi'(Z)$ and $\psi(Z)$ in equation(6), the stress field over the crack tip, (x=a) is then calculated:

$$\sigma_{xx}+\sigma_{yy}=2\left[\phi(Z)+\overline{\phi(Z)}\right]=\frac{1}{\pi}\left[\frac{P}{\sqrt{2ar}}\sqrt{\frac{a+s}{a-s}}\cos\frac{\theta}{2}-\frac{Q}{\sqrt{2ar}}\sqrt{\frac{a+s}{a-s}}\sin\frac{\theta}{2}-\frac{Q}{a-s}\right] \quad (14)$$

$$\sigma_{xx}-\sigma_{yy}+2i\sigma_{xy}=2\left[(\overline{Z}-Z).\phi'(Z)-\phi(Z)+\overline{\psi(Z)}\right]$$
$$=\frac{1}{\pi}\left[\frac{P}{\sqrt{2ar}}\sqrt{\frac{a+s}{a-s}}\left(\cos\frac{\theta}{2}\sin\frac{\theta}{2}\sin\frac{3\theta}{2}\right)+\frac{Q}{\sqrt{2ar}}\sqrt{\frac{a+s}{a-s}}\left(\sin\frac{\theta}{2}\cos\frac{\theta}{2}\cos\frac{3\theta}{2}\right)+\frac{Q}{a-s}\right] \quad (15)$$
$$+\frac{i}{\pi}\left[\frac{P}{\sqrt{2ar}}\sqrt{\frac{a+s}{a-s}}\sin\frac{\theta}{2}\left(1+\cos\frac{\theta}{2}\cos\frac{3\theta}{2}\right)+\frac{Q}{\sqrt{2ar}}\sqrt{\frac{a+s}{a-s}}\cos\frac{\theta}{2}\left(1-\sin\frac{\theta}{2}\sin\frac{3\theta}{2}\right)\right]$$

Finally, stresses can be calculated as follows:

$$\sigma_{xx}=\frac{1}{2\pi}\left[\frac{P}{\sqrt{2ar}}\sqrt{\frac{a+s}{a-s}}\cos\frac{\theta}{2}-\frac{Q}{\sqrt{2ar}}\sqrt{\frac{a+s}{a-s}}\sin\frac{\theta}{2}-\frac{Q}{a-s}\right]$$
$$+\frac{1}{2\pi}\left[\frac{P}{\sqrt{2ar}}\sqrt{\frac{a+s}{a-s}}\left(\cos\frac{\theta}{2}\sin\frac{\theta}{2}\sin\frac{3\theta}{2}\right)+\frac{Q}{\sqrt{2ar}}\sqrt{\frac{a+s}{a-s}}\left(\sin\frac{\theta}{2}\cos\frac{\theta}{2}\cos\frac{3\theta}{2}\right)+\frac{Q}{a-s}\right]\rightarrow \quad (16)$$
$$\sigma_{xx}=\frac{1}{2\pi\sqrt{2ar}}\sqrt{\frac{a+s}{a-s}}\left[P\cos\frac{\theta}{2}\left(1+\sin\frac{\theta}{2}\sin\frac{3\theta}{2}\right)-Q\sin\frac{\theta}{2}\left(1-\cos\frac{\theta}{2}\cos\frac{3\theta}{2}\right)\right]$$

$$\sigma_{yy}=\frac{1}{2\pi\sqrt{2ar}}\sqrt{\frac{a+s}{a-s}}\left[P\cos\frac{\theta}{2}\left(1-\sin\frac{\theta}{2}\sin\frac{3\theta}{2}\right)-Q\sin\frac{\theta}{2}\left(1-\cos\frac{\theta}{2}\cos\frac{3\theta}{2}\right)\right]-\frac{Q}{\pi(a-s)} \quad (17)$$

$$\sigma_{xy}=\frac{1}{2\pi\sqrt{2ar}}\sqrt{\frac{a+s}{a-s}}\left[P\sin\frac{\theta}{2}\left(1+\cos\frac{\theta}{2}\cos\frac{3\theta}{2}\right)+Q\cos\frac{\theta}{2}\left(1-\sin\frac{\theta}{2}\sin\frac{3\theta}{2}\right)\right] \tag{18}$$

As mentioned before, φ and ψ are useful for describing the effect of shear stress; therefore based on these equations, the stress intensity factor in Mode II can be achieved. Once established, stress intensity factor at (x=a) could be calculated as:

$$K_{II}^{A}=\lim_{\substack{\theta\to 0\\ x\to 0}}\sqrt{2\pi r}\,\sigma_{12}=\frac{Q}{2\sqrt{\pi a}}\sqrt{\frac{a+s}{a-s}} \tag{19}$$

4. Stress Field and Stress Intensity Factor Determination (Mode II) (x=-a)

According to Figure 3 and Figure 4, it is assumed in (x=-a) such that $Z=-(a+\xi)$, $\xi=re^{i\theta}$ and $\left|\frac{\xi}{a}\right|<<1$, then:

$$\phi(Z)=\frac{P-iQ}{4\pi i(Z-s)}\left[\sqrt{\frac{s^2-a^2}{Z^2-a^2}}+1\right]=-\frac{P-iQ}{4\pi i}\left[\frac{i}{\sqrt{2a\xi}}\sqrt{\frac{a-s}{a+s}}+\frac{1}{a+s}\right] \tag{20}$$

Substituting $\xi=re^{i\theta}$;

$$\begin{aligned}\phi(Z)=&\frac{1}{4\pi}\left[\frac{-P}{\sqrt{2ar}}\sqrt{\frac{a-s}{a+s}}\cos\frac{\theta}{2}+\frac{Q}{\sqrt{2ar}}\sqrt{\frac{a-s}{a+s}}\sin\frac{\theta}{2}+\frac{Q}{a+s}\right]\\&+\frac{i}{4\pi}\left[\frac{P}{\sqrt{2ar}}\sqrt{\frac{a-s}{a+s}}\sin\frac{\theta}{2}+\frac{Q}{\sqrt{2ar}}\sqrt{\frac{a-s}{a+s}}\cos\frac{\theta}{2}+\frac{P}{a+s}\right]\end{aligned} \tag{21}$$

By differentiating (21) on ξ, it follows:

$$\phi'(Z)=\frac{d\phi}{dZ}=\frac{d}{d\xi}\left\{-\frac{P-iQ}{4\pi i}\left[\frac{i}{\sqrt{2a\xi}}\sqrt{\frac{a-s}{a+s}}+\frac{1}{a+s}\right]\right\}=-\frac{P-iQ}{4\pi}\left[\frac{-1}{2\sqrt{2a\xi^3}}\sqrt{\frac{a-s}{a+s}}\right] \tag{22}$$

Substituting $\xi=re^{i\theta}$;

$$\phi'(Z)=\frac{1}{4\pi}\frac{1}{2r\sqrt{2ar}}\sqrt{\frac{a-s}{a+s}}\left[\left(P\cos\frac{3\theta}{2}-Q\sin\frac{3\theta}{2}\right)-i\left(P\sin\frac{3\theta}{2}+Q\cos\frac{3\theta}{2}\right)\right] \tag{23}$$

$\psi(Z)$ is to be solved considering the same condition used for $\phi(Z)$ at (x=-a):

$$\psi(Z)=\frac{P-iQ}{4\pi i(Z-s)}\left[\sqrt{\frac{s^2-a^2}{Z^2-a^2}}-1\right]=-\frac{P-iQ}{4\pi}\left[\frac{1}{\sqrt{2a\xi}}\sqrt{\frac{a-s}{a+s}}+\frac{i}{a+s}\right] \tag{24}$$

Substituting $\xi=re^{i\theta}$;

$$\psi(Z)=\frac{1}{4\pi}\left[\frac{-P}{\sqrt{2ar}}\sqrt{\frac{a-s}{a+s}}\cos\frac{\theta}{2}+\frac{Q}{\sqrt{2ar}}\sqrt{\frac{a-s}{a+s}}\sin\frac{\theta}{2}-\frac{Q}{a+s}\right]$$
$$+\frac{i}{4\pi}\left[\frac{P}{\sqrt{2ar}}\sqrt{\frac{a-s}{a+s}}\sin\frac{\theta}{2}+\frac{Q}{\sqrt{2ar}}\sqrt{\frac{a-s}{a+s}}\cos\frac{\theta}{2}-\frac{P}{a+s}\right] \quad (25)$$

Here, by substituting values of $\phi(Z)$, $\phi'(Z)$ and $\psi(Z)$ in equation (6), stress field over crack tip (x=-a) is then calculated:

$$\sigma_{xx}+\sigma_{yy}=2\left[\phi(Z)+\overline{\phi(Z)}\right]=\frac{1}{\pi}\left[\frac{-P}{\sqrt{2ar}}\sqrt{\frac{a-s}{a+s}}\cos\frac{\theta}{2}+\frac{Q}{\sqrt{2ar}}\sqrt{\frac{a-s}{a+s}}\sin\frac{\theta}{2}+\frac{Q}{a+s}\right] \quad (26)$$

$$\sigma_{xx}-\sigma_{yy}+2i\sigma_{xy}=2\left[(\overline{Z}-Z).\phi'(Z)-\phi(Z)+\overline{\psi(Z)}\right]$$
$$=\frac{-1}{\pi}\left[\frac{P}{\sqrt{2ar}}\sqrt{\frac{a-s}{a+s}}\left(\cos\frac{\theta}{2}\sin\frac{\theta}{2}\sin\frac{3\theta}{2}\right)+\frac{Q}{\sqrt{2ar}}\sqrt{\frac{a-s}{a+s}}\left(\sin\frac{\theta}{2}\cos\frac{\theta}{2}\cos\frac{3\theta}{2}\right)+\frac{Q}{a+s}\right] \quad (27)$$
$$-\frac{i}{\pi}\left[\frac{P}{\sqrt{2ar}}\sqrt{\frac{a-s}{a+s}}\sin\frac{\theta}{2}\left(1+\cos\frac{\theta}{2}\cos\frac{3\theta}{2}\right)+\frac{Q}{\sqrt{2ar}}\sqrt{\frac{a-s}{a+s}}\cos\frac{\theta}{2}\left(1-\sin\frac{\theta}{2}\sin\frac{3\theta}{2}\right)\right]$$

Finally, stresses can be calculated as follows:

$$\sigma_{xx}=\frac{1}{2\pi}\left[\frac{-P}{\sqrt{2ar}}\sqrt{\frac{a-s}{a+s}}\cos\frac{\theta}{2}+\frac{Q}{\sqrt{2ar}}\sqrt{\frac{a-s}{a+s}}\sin\frac{\theta}{2}+\frac{Q}{a+s}\right]$$
$$-\frac{1}{2\pi}\left[\frac{P}{\sqrt{2ar}}\sqrt{\frac{a-s}{a+s}}\left(\cos\frac{\theta}{2}\sin\frac{\theta}{2}\sin\frac{3\theta}{2}\right)+\frac{Q}{\sqrt{2ar}}\sqrt{\frac{a-s}{a+s}}\left(\sin\frac{\theta}{2}\cos\frac{\theta}{2}\cos\frac{3\theta}{2}\right)+\frac{Q}{a+s}\right]\rightarrow \quad (28)$$
$$\sigma_{xx}=\frac{1}{2\pi\sqrt{2ar}}\sqrt{\frac{a-s}{a+s}}\left[-P\cos\frac{\theta}{2}\left(1+\sin\frac{\theta}{2}\sin\frac{3\theta}{2}\right)+Q\sin\frac{\theta}{2}\left(1+\cos\frac{\theta}{2}\cos\frac{3\theta}{2}\right)\right]$$

$$\sigma_{yy}=\frac{1}{2\pi\sqrt{2ar}}\sqrt{\frac{a-s}{a+s}}\left[-P\cos\frac{\theta}{2}\left(1-\sin\frac{\theta}{2}\sin\frac{3\theta}{2}\right)+Q\sin\frac{\theta}{2}\left(1+\cos\frac{\theta}{2}\cos\frac{3\theta}{2}\right)\right]+\frac{Q}{\pi(a+s)} \quad (29)$$

$$\sigma_{xy}=\frac{-1}{2\pi\sqrt{2ar}}\sqrt{\frac{a-s}{a+s}}\left[P\sin\frac{\theta}{2}\left(1+\cos\frac{\theta}{2}\cos\frac{3\theta}{2}\right)+Q\cos\frac{\theta}{2}\left(1-\sin\frac{\theta}{2}\sin\frac{3\theta}{2}\right)\right] \quad (30)$$

As mentioned before, φ and ψ are useful in describing the effect of shear stress; therefore based on these equations, stress intensity factor in Mode II could be achieved. Once established, the stress intensity factor at (x=-a) could be calculated as:

$$\frac{P}{2\sqrt{\pi a}}\sqrt{\frac{a-s}{a+s}} \quad (31)$$

As mentioned, equation) cannot describe P force for Mode I and equation (32) is used:

$$\phi(Z)=\frac{P.\sqrt{a^2-s^2}}{\pi(Z-s).\sqrt{Z^2-s^2}} \tag{32}$$

Consideration of proposed ϕ by Irwin stress field in an infinite region could be as follows:

$$\begin{aligned}\sigma_{xx}&=\mathrm{Re}\,\phi(Z)-y.\mathrm{Im}\,\phi'(Z)\\ \sigma_{yy}&=\mathrm{Re}\,\phi(Z)+y.\mathrm{Im}\,\phi'(Z)\\ \sigma_{xy}&=-y.\mathrm{Re}\,\phi'(Z)\end{aligned} \tag{33}$$

5. Stress Field and Stress Intensity Factor Determination (Mode I) (x=a)

In order to determine stress field and stress intensity factor in Mode I, according to Figure 3 and Figure 4, it is assumed in (x=a) such that $Z=a+\xi$, $\xi=re^{i\theta}$ and $\left|\frac{\xi}{a}\right|<<1$, then:

$$\phi(Z)=\frac{P\sqrt{a^2-s^2}}{\pi(Z-s).\sqrt{Z^2-a^2}}=\frac{P\sqrt{a^2-s^2}}{\pi\sqrt{(\xi^2+(a-s)^2+2a\xi(a-s))(\xi^2+2a\xi)}} \tag{34}$$

Considering $\xi\to 0$ at crack tip, the power terms of crack tip would be negligible;

$$\phi(Z)=\frac{P}{\pi\sqrt{2a\xi}}\sqrt{\frac{a+s}{a-s}} \tag{35}$$

Substituting $\xi=re^{i\theta}$;

$$\phi(Z)=\frac{P}{\pi\sqrt{2ar}}\sqrt{\frac{a+s}{a-s}}\left(\cos\frac{\theta}{2}-i\sin\frac{\theta}{2}\right) \tag{36}$$

By differentiating (35) on ξ, it follows:

$$\phi'(Z)=\frac{d\phi}{dZ}=\frac{d}{d\xi}\left[\frac{P}{\pi\sqrt{2a\xi}}\sqrt{\frac{a+s}{a-s}}\right]=\frac{-P}{2\pi\sqrt{2a\xi^3}}\sqrt{\frac{a+s}{a-s}} \tag{37}$$

Substituting $\xi=re^{i\theta}$;

$$\phi'(Z)=\frac{-P}{2\pi r\sqrt{2ar}}\sqrt{\frac{a+s}{a-s}}\left(\cos\frac{3\theta}{2}-i\sin\frac{3\theta}{2}\right) \tag{38}$$

Here, by substituting values of $\phi(Z)$ and $\phi'(Z)$ in equation (33), stress field over crack tip (x=a) is then calculated:

$$\begin{aligned}\sigma_{xx}&=\mathrm{Re}\,\phi(Z)-y.\mathrm{Im}\,\phi'(Z)=\frac{P}{\pi\sqrt{2ar}}\sqrt{\frac{a+s}{a-s}}\cos\frac{\theta}{2}-\frac{P}{\pi\sqrt{2ar}}\sqrt{\frac{a+s}{a-s}}\cos\frac{\theta}{2}\sin\frac{\theta}{2}\sin\frac{3\theta}{2}\\ &=\frac{P}{\pi\sqrt{2ar}}\sqrt{\frac{a+s}{a-s}}\cos\frac{\theta}{2}\left(1-\sin\frac{\theta}{2}\sin\frac{3\theta}{2}\right)\end{aligned} \tag{39}$$

$$\sigma_{yy} = \mathrm{Re}\,\phi(Z) + y.\mathrm{Im}\,\phi'(Z) = \frac{P}{\pi\sqrt{2ar}}\sqrt{\frac{a+s}{a-s}}\cos\frac{\theta}{2} + \frac{P}{\pi\sqrt{2ar}}\sqrt{\frac{a+s}{a-s}}\cos\frac{\theta}{2}\sin\frac{\theta}{2}\sin\frac{3\theta}{2}$$
$$= \frac{P}{\pi\sqrt{2ar}}\sqrt{\frac{a+s}{a-s}}\cos\frac{\theta}{2}\left(1+\sin\frac{\theta}{2}\sin\frac{3\theta}{2}\right) \quad (40)$$

$$\sigma_{xy} = -y.\mathrm{Re}\,\phi'(Z) = \frac{P}{\pi\sqrt{2ar}}\sqrt{\frac{a+s}{a-s}}\sin\frac{\theta}{2}\cos\frac{\theta}{2}\cos\frac{3\theta}{2} \quad (41)$$

Considering the presented ϕ, which is useful in obtaining the stress intensity factor in Mode I, SIF at (x=a) could be calculated as:

$$K_I^A = \sqrt{2\pi r}\sigma_{22} = \sqrt{2\pi r}\left(\frac{P}{\pi\sqrt{2ar}}\sqrt{\frac{a+s}{a-s}}\cos\frac{\theta}{2}\left(1+\sin\frac{\theta}{2}\sin\frac{3\theta}{2}\right)\right)\xrightarrow{\theta=0}$$
$$K_I^A = \frac{P}{\sqrt{\pi a}}\sqrt{\frac{a+s}{a-s}} \quad (42)$$

6. Stress Field and Stress Intensity Factor Determination (Mode I) (X=-A)

According to Figure 3 and Figure 4, it is assumed in (x=-a) such that $Z = -(a+\xi)$, $\xi = re^{i\theta}$ and $\left|\frac{\xi}{a}\right| << 1$, then:

$$\phi(Z) = \frac{P\sqrt{a^2-s^2}}{\pi(Z-s).\sqrt{Z^2-a^2}} = \frac{P\sqrt{a^2-s^2}}{\pi\sqrt{(\xi^2+(a+s)^2+2a\xi(a+s))(\xi^2+2a\xi)}} \quad (43)$$

Considering $\xi \to 0$ at crack tip, therefore power terms of crack tip would be negligible;

$$\phi(Z) = \frac{P}{\pi\sqrt{2a\xi}}\sqrt{\frac{a-s}{a+s}} \quad (44)$$

Substituting $\xi = re^{i\theta}$;

$$\phi(Z) = \frac{P}{\pi\sqrt{2ar}}\sqrt{\frac{a-s}{a+s}}\left(\cos\frac{\theta}{2} - i\sin\frac{\theta}{2}\right) \quad (45)$$

By differentiating (44) on ξ, it follows:

$$\phi'(Z) = \frac{d\phi}{dZ} = \frac{d}{d\xi}\left[\frac{P}{\pi\sqrt{2a\xi}}\sqrt{\frac{a-s}{a+s}}\right] = \frac{-P}{2\pi\sqrt{2a\xi^3}}\sqrt{\frac{a-s}{a+s}} \quad (46)$$

Substituting $\xi = re^{i\theta}$;

$$\phi'(Z) = \frac{-P}{2\pi r\sqrt{2ar}}\sqrt{\frac{a-s}{a+s}}\left(\cos\frac{3\theta}{2} - i\sin\frac{3\theta}{2}\right) \quad (47)$$

Here, by substituting values of $\phi(Z)$ and $\phi'(Z)$ in equation (33), stress field over crack tip (x=-a) is then calculated:

$$\sigma_{xx} = \mathrm{Re}\,\phi(Z) - y.\mathrm{Im}\,\phi'(Z) = \frac{P}{\pi\sqrt{2ar}}\sqrt{\frac{a-s}{a+s}}\cos\frac{\theta}{2} - \frac{P}{\pi\sqrt{2ar}}\sqrt{\frac{a-s}{a+s}}\cos\frac{\theta}{2}\sin\frac{\theta}{2}\sin\frac{3\theta}{2}$$
$$= \frac{P}{\pi\sqrt{2ar}}\sqrt{\frac{a-s}{a+s}}\cos\frac{\theta}{2}\left(1-\sin\frac{\theta}{2}\sin\frac{3\theta}{2}\right) \quad (48)$$

$$\sigma_{yy} = \mathrm{Re}\,\phi(Z) + y.\mathrm{Im}\,\phi'(Z) = \frac{P}{\pi\sqrt{2ar}}\sqrt{\frac{a-s}{a+s}}\cos\frac{\theta}{2} + \frac{P}{\pi\sqrt{2ar}}\sqrt{\frac{a-s}{a+s}}\cos\frac{\theta}{2}\sin\frac{\theta}{2}\sin\frac{3\theta}{2}$$
$$= \frac{P}{\pi\sqrt{2ar}}\sqrt{\frac{a-s}{a+s}}\cos\frac{\theta}{2}\left(1+\sin\frac{\theta}{2}\sin\frac{3\theta}{2}\right) \quad (49)$$

Stress intensity factor at (x=-a) could be calculated as:

$$K_I^B = \sqrt{2\pi r}\sigma_{22} = \sqrt{2\pi r}\left(\frac{P}{\pi\sqrt{2ar}}\sqrt{\frac{a-s}{a+s}}\cos\frac{\theta}{2}\left(1+\sin\frac{\theta}{2}\sin\frac{3\theta}{2}\right)\right) \xrightarrow{\theta=0}$$
$$K_I^B = \frac{P}{\sqrt{\pi a}}\sqrt{\frac{a-s}{a+s}} \quad (50)$$

7. Model Description

Numerical simulation of the problem has been carried out using the finite element method, since there are no analytical solutions of similar problems and no possibility to perform empirical tests. Model geometry includes a Brazilian disc containing two cracks with orientations of 0 and 90 degrees (Fig. 5). Considering ISRM standard, the radius and thickness of the disc are considered to be 54 and 27 millimetres, respectively. SIF has thus been calculated for three different angles of 0 and 90 degrees, the results of which are shown in Table 2.

Stress concentration near the crack tip has been numerically presented as shown in Figure 6.

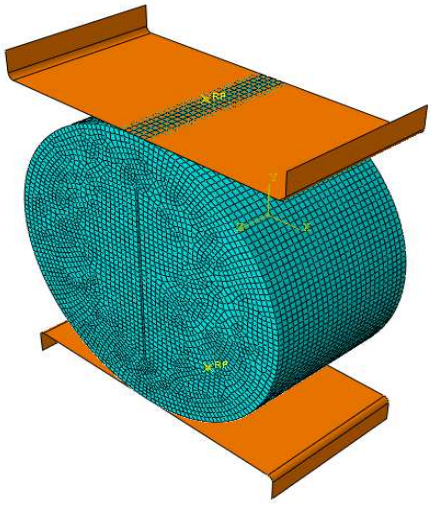

Fig. 5. Schematic FE model with a crack orientation of 0 degrees.

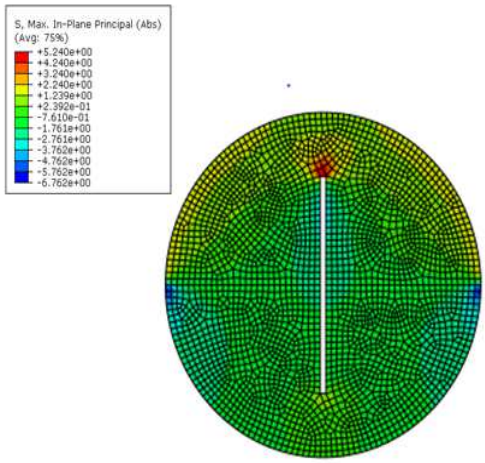

Fig. 6. Stress concentration near the crack tips.

8. Results and Discussions

In summary, the results obtained from the solution for different angles shall be summarized as Table 1:

Table 1. The results obtained from analytical solution.

Angles (degree)	0	90
K_I^A	$\frac{P}{\sqrt{\pi a}}\sqrt{\frac{a+s}{a-s}}$	$\frac{3\sqrt{2}P}{4\sqrt{\pi a}}\sqrt{\frac{a+s}{a-s}}$
K_{II}^A	$\frac{Q}{2\sqrt{\pi a}}\sqrt{\frac{a+s}{a-s}}$	$\frac{1}{4\sqrt{2\pi a}}\sqrt{\frac{a+s}{a-s}}[P+Q]$
K_I^B	$\frac{P}{\sqrt{\pi a}}\sqrt{\frac{a-s}{a+s}}$	$\frac{3\sqrt{2}P}{4\sqrt{\pi a}}\sqrt{\frac{a-s}{a+s}}$
K_{II}^B	$\frac{Q}{2\sqrt{\pi a}}\sqrt{\frac{a-s}{a+s}}$	$\frac{1}{4\sqrt{2\pi a}}\sqrt{\frac{a-s}{a+s}}[P+Q]$

By substituting numeric equivalents for P, Q, a, and s, presented in Table 1, along with the results of numerical modelling, dimensionless values for K1 and K2 were obtained as provided in Table 2 (a/R=0.6).

Table 2. The comparison between the results of analytical solution and numerical modelling.

Angles (degree)	0		90	
Method	Analytical solution	Numerical modelling	Analytical solution	Numerical modelling
K_I^A / K_{IC}	1.014	0.913	0.987	1.014
K_{II}^A / K_{IIC}	0.897	0.985	1.131	1.021
K_I^B / K_{IC}	1.021	0.986	0.893	0.954
K_{II}^B / K_{IIC}	0.987	1.013	0.934	1.148

According to the results showed in table 2, it can be seen that results of analytical solution and numerical modelling are in good agreement.

9. Conclusions

The two chevron-notched rock fracture specimens, chevron bend (CB) and short rod (SR), recommended by the ISRM to determine rock Mode I fracture toughness, have a number of practical disadvantages such as low loads required to initiate failure at the correct orientation, complicated loading fixtures, and complex sample preparation for CB and SR specimens. The cracked chevron-notched Brazilian disc (CCNBD) and the cracked straight-through Brazilian disc (CSTBD) specimen geometries overcome these problems. CCNBD is an ideal specimen geometry for rock Mode I fracture toughness, while the CSTBD is an ideal specimen to be used for mixed Mode I and II fracture studies such as Mode II fracture toughness measurement, rock fracture strength locus tests, and rock mixed mode crack propagation investigations. Good features of CSTBD are

high failure load, simple loading fixture, and convenient and flexible specimen preparation. In this paper, stress field and stress intensity factor for CSTBD specimens have been theoretically presented. In addition, the analytical solution has been compared with numerical modelling results, showing the same outcome for both methods. Finally, it should be mentioned that the proposed method thus remains valid for any crack of arbitrary length and angle. The results demonstrate that the magnitude of critical load in structures that prevent cracks from initiation shall be identified.

References

[1] Fowell, R.J. (1995). Suggested method for determining mode I fracture toughness using cracked chevron notched Brazilian disc (CCNBD) specimens, International Journal of Rock Mechanics and Mining Sciences & Geomechanics Abstracts, pp. 57-64.

[2] Iqbal, M. and Mohanty, B. (2006). Experimental calibration of stress intensity factors of the ISRM suggested cracked chevron-notched Brazilian disc specimen used for determination of mode-I fracture toughness, International Journal of Rock Mechanics and Mining Sciences, 43, pp. 1270-1276.

[3] Fowell, R. and Chen, J. (1990). The third chevron-notch rock fracture specimen—the cracked chevron-notched Brazilian disk, Proc. 31st US Symp. Rock. Balkema, Rotterdam, pp. 295-302.

[4] Chen, J. (1990). The development of the cracked-chevron-notched Brazilian disc methods for rock fracture toughness measurement, Proceeding of 1990 SEM Spring Conference on Experimental Mechanics, pp. 18-23.

[5] Fowell, R. and Xu, C. (1993). The cracked chevron notched Brazilian disc test-geometrical considerations for practical rock fracture toughness measurement, International Journal of Rock Mechanics and Mining Sciences & Geomechanics abstracts, pp. 821-824.

[6] Xu, C., and Fowell, R., (1994). Stress intensity factor evaluation for cracked chevron notched Brazilian disc specimens, International Journal of Rock Mechanics and Mining Sciences & Geomechanics Abstracts, pp. 157-162.

[7] Wang, Q.Z. (1998). Stress intensity factors of the ISRM suggested CCNBD specimen used for mode-I fracture toughness determination, International Journal of Rock Mechanics and Mining Sciences, 35, pp. 977-982.

[8] Wang, Q., Jia, X., Kou, S., Zhang, Z. and Lindqvist, P.A. (2003). More accurate stress intensity factor derived by finite element analysis for the ISRM suggested rock fracture toughness specimen—CCNBD, International Journal of Rock Mechanics and Mining Sciences, 40, pp. 233-241.

[9] Wang, Q., Jia, X. and Wu, L. (2004). Wide-range stress intensity factors for the ISRM suggested method using CCNBD specimens for rock fracture toughness tests, International Journal of Rock Mechanics and Mining Sciences, 41, pp. 709-716.

[10] Wang, Q. (2010). Formula for calculating the critical stress intensity factor in rock fracture toughness tests using cracked chevron notched Brazilian disc (CCNBD) specimens, International Journal of Rock Mechanics and Mining Sciences, 47, pp. 1006-1011.

[11] Wang, Q., Fan, H., Gou, X. and Zhang, S. (2013). Recalibration and Clarification of the Formula Applied to the ISRM-Suggested CCNBD Specimens for Testing Rock Fracture Toughness, Rock Mechanics and Rock Engineering, 46, pp. 303-313.

[12] Barker, L. (1977). A simplified method for measuring plane strain fracture toughness, Engineering Fracture Mechanics, 9, pp. 361-369.

[13] Ouchterlony, F. (1988). Suggested methods for determining the fracture toughness of rock, International Journal of Rock Mechanics and Mining Sciences, 25, pp. 71-96.

[14] Awaji, H. and Sato, S. (1978). Combined mode fracture toughness measurement by the disk test, Journal of Engineering Materials and Technology, 100, p. 175.

[15] Sheity, D.K., Rosenfield, A.R. and Duckworth, W.H. (1985). Fracture Toughness of Ceramics Measured by a Chevron-Notch Diametral-Compression Test, Journal of the American Ceramic Society, 68, pp. C-325-C-327.

[16] Rooke, D. and Tweed, J. (1973). The stress intensity factors of a radial crack in a point loaded disc, International Journal of Engineering Science, 11, pp. 285-290.

[17] Atkinson, C., Smelser, R. and Sanchez, J. (1982). Combined mode fracture via the

cracked Brazilian disk test, International Journal of Fracture, 18, pp. 279-291.

[18]Timoshenko, S. and Goodier, J. (1970). Theory of elasticity, 3rd Edition, New York: McGraw-Hill.

[19] Xu, C. (1993). Rock fracture mechanics and excavation engineering, Unpublished PhD. thesis, University of Leeds.

[20] Erdogan, F. (1962). On the stress distribution in plates with collinear cuts under arbitrary loads, Proceedings of the Fourth US National Congress of Applied Mechanics, pp. 547-553.

[21] Fowell, R. and Xu, C. (1994). The use of the cracked Brazilian disc geometry for rock fracture investigations, International Journal of Rock Mechanics and Mining Sciences & Geomechanics Abstracts, pp. 571-579.